FOR PEER REVIEW - CONFIDENTIAL

Ongoing fragmentation of the subducting Cocos slab

Tracking no: G51403

Authors:

Tu Xue (Missouri University of Science and Technology), Diandian Peng (University of Illinois at Urbana-Champaign), Kelly Liu (Missouri University of Science and Technology), Jonathan Obrist-Farner (Missouri University of Science and Technology), Marek Locmelis (Missouri University of Science and Technology), Stephen Gao (Missouri University of Science and Technology), and Lijun Liu (University of Illinois at Urbana-Champaign)

Abstract:

Fundamental to plate tectonics is the subduction of cold and mechanically strong oceanic plates. While the subducted plates are conventionally regarded to be impermeable to mantle flow that separate the mantle wedge and the subslab region, isolated openings (termed slab gaps hereinafter) have been proposed. Here, by combining new shear wave splitting measurements with results from geodynamic modeling and recent seismic tomography and geochemical observations, we show that the upper ~200 km of the Cocos slab in northern Central America is intensively fractured. It is strong enough to produce typical arc volcanoes and Benioff Zone earthquakes but allows mantle flow to traverse from the subslab region to the mantle wedge. Upwelling of hot subslab mantle flow through the slab provides a viable explanation for the behind-the-arc volcanoes that are geochemically distinct from typical arc volcanoes, and for the puzzling high heat flow, high elevation, and low Bouguer gravity anomalies observed in the area.

Ongoing fragmentation of the subducting Cocos slab

- Tu Xue¹, Diandian Peng², Kelly H. Liu¹, Jonathan Obrist-Farner¹, Marek Locmelis¹, Stephen S. Gao¹*, and Lijun Liu²*
- ¹Geology and Geophysics Program, Missouri University of Science and Technology; Rolla, MO
- 5 65401, USA.
- 6 ²Department of Geology, University of Illinois at Urbana-Champaign; Champaign, IL 61801,
- 7 USA.

1

- *Corresponding author. Email: sgao@mst.edu;
- 9 *Corresponding author. Email: <u>liliu@illinois.edu</u>
- 10 ABSTRACT
- 11 Fundamental to plate tectonics is the subduction of cold and mechanically strong oceanic
- plates. While the subducted plates are conventionally regarded to be impermeable to
- mantle flow that separate the mantle wedge and the subslab region, isolated openings
- 14 (termed slab gaps hereinafter) have been proposed. Here, by combining new shear wave
- splitting measurements with results from geodynamic modeling and recent seismic
- tomography and geochemical observations, we show that the upper ~200 km of the Cocos
- slab in northern Central America is intensively fractured. It is strong enough to produce
- 18 typical arc volcanoes and Benioff Zone earthquakes but allows mantle flow to traverse
- 19 from the subslab region to the mantle wedge. Upwelling of hot subslab mantle flow through
- 20 the slab provides a viable explanation for the behind-the-arc volcanoes that are
- 21 geochemically distinct from typical arc volcanoes, and for the puzzling high heat flow, high
- 22 elevation, and low Bouguer gravity anomalies observed in the area.

INTRODUCTION

- The Cocos Plate is bounded by the East Pacific Rise on the west and the Galapagos
- 25 spreading center to the south (Fig. 1). It was formed when the Farallon Plate broke into two
- pieces approximately 23 million years ago (Pardo and Suárez, 1995; Dougherty et al., 2012;

Borgeaud et al., 2019). Compared with most other regions with convergent plate boundary zones, northern Central America, where the Cocos Plate is subducting beneath the North American and Caribbean plates, has several puzzling observations including anomalously high topography (Rogers et al, 2002), high heat flow (Blackwell et al., 1990), low Bouguer gravity anomalies (Fig. S1), and the presence of intraplate Cenozoic volcanoes in eastern Guatemala and western El Salvador (Fig. 1). A compilation of measurements from existing geochemical studies indicates that the primitive-mantle-normalized trace element patterns from samples from the volcanic front (VF) and behind the volcanic front (BVF) are notably different (Fig. 2A). The VF lavas display features commonly associated with hydrous magmas derived from a subducting slab, most notably a distinct negative Nb and Ta anomalies (Baier et al., 2008). Conversely, the absence of negative Nb and Ta anomalies in the BVF lavas, combined with elevated contents of light rare earth elements that display a steeper decline from La to Sm when compared to VF, suggest that the BVF lavas formed from partial melting of a protolith without significant water content. Another unusual feature of this area is the lack of deep-focus earthquakes and a reduction in earthquake productivity in the depth range of ~100-200 km relative to the other subduction zones (Fig. 2B).

27

28

29

30

31

32

33

34

35

36

37

38

39

40

41

42

43

44

45

46

47

48

49

Mostly due to poor coverage by seismic stations in the area and the resulting low resolution of seismic tomographic images, conflicting conclusions regarding the continuity and geometry of the Cocos slab have been reached by different tomography studies. Based on a global-scale P-wave velocity model, Rogers (2002) proposed the existence of a slab gap in the depth range of 200-500 km that horizontally extends for ~900 km from southern Mexico to Honduras. They attributed the high elevation in the back-are area to upwelling mantle flow through this slab gap. This model, however, is inconsistent with more recent tomographic images.

For instance, a regional-scale full-waveform inversion study (Zhu et al, 2020) revealed a continuous Cocos slab extending from the surface to a depth of at least 1000 km. The same study also found that in the top 200 km, the velocity anomaly of the slab is significantly weaker than that in deeper sections of the slab (Fig. S2), consistent with the reduced seismicity around this depth (Fig. 2B). Additionally, at depths greater than 80 km, the dominant fast orientation of seismic anisotropy, which represents the mantle flow direction in the sublithospheric mantle, is different between the oceanic and continental sides. Specifically, it is trench perpendicular on the Cocos side and becomes E-W on the Caribbean side with a clear right-turn pattern (Fig. S3). As detailed below, such a pattern of fast orientations can be explained by a mantle flow system traversing from the subslab region to the mantle wedge across the fragmenting Cocos slab.

CONSTRAINTS ON THE MANTLE FLOW FIELDS FROM SHEAR

WAVE SPLITTING ANALYSIS

In addition to seismic tomography, numerous studies have demonstrated that the mantle flow system in the vicinity of a subducting slab can be delineated by analyzing the splitting of shear waves (Hess, 1964; Silver and Chan 1991; Long and Silver, 2009; Zhou et al., 2018; Kong et al., 2018). Relative to seismic tomography, shear wave splitting analysis (see Methods) has a higher lateral and lower vertical resolution. In Nicaragua and Costa Rica, which are located to the southeast of the study area, the fast orientations from shear wave splitting analysis are largely trench parallel and can be interpreted to reflect along-trench flow in the mantle wedge and beneath the slab (Abt et al., 2010). In contrast, the fast orientations in southern Mexico are dominantly trench perpendicular and are interpreted as reflecting subduction-induced corner flow in the mantle wedge (Bernal-López et al., 2016) (Fig. 1), as pervasively observed in other subduction zones worldwide (Long and Silver, 2009).

The fast orientations from shear wave splitting analysis for the Caribbean Plate are neither trench parallel nor trench perpendicular (Fig. 3). More intriguingly, observations at stations located on the southwestern side of the volcanic arc show a clear dependence on the arriving azimuth of the seismic waves. In particular, the fast orientations tend to be more trench perpendicular for ray paths arriving at the stations from the southwest (and thus sample the ocean side of the mantle) than those from other back-azimuths. This pattern is consistent with a clockwise rotation of the inferred mantle flow directions that is also revealed by results from a full-waveform inversion (Zhu et al., 2020) (Fig. S3). Another notable feature is a sudden change in anisotropy orientations across the North American-Caribbean Plate boundaries, where results in the northern part are more trench-normal that resembles typical wedge flow. This implies an abnormal flow pattern below the Caribbean Plate in western Central America.

NUMERICAL SIMULATION OF CENOZOIC COCOS SUBDUCTION

To quantitatively evaluate the subduction dynamics of the Cocos plate, we perform numerical models with data-assimilation (Liu and Stegman, 2011) that satisfy the observed Cenozoic plate motion history and sea floor ages (see Methods). Tests show that simulations starting no later than 40 Ma produce similar present-day slab structures at < 800 km depth. Our results from a case study that covers subduction since 45 Ma show that below the study area, the central portion of the Cocos slab experienced gradual shallowing since ~30 Ma and eventually developed a central slab tear along the slab hinge toward the present (Fig. 4). The resulting present slab geometry, including both a highly extended thin slab with multiple slab holes above 200 km depth and the folded slab pile further down (Fig. 4E), matches the shear wave splitting measurements (Fig. 3) and recent seismic tomographic results well (Fig. 4F).

Physically, the progressive dip angle reduction leading to the present fragmenting slab below our study region reflects the sub-slab pressure accumulation over time: the finite width of the Cocos Plate allows the sub-slab pressure to be released around the northern and southern edges of the slab but not in the center. Consequently, the reduced slab dip angle is a result of the enhanced pressure gradient across the slab below the western part of the Caribbean Plate. The fast-retreating northern Cocos trench since 30 Ma further enhanced this N-S contrasting slab movement, facilitating slab flattening and deformation in the study region. Slab buckling with potential fracturing started to develop along the slab hinge at ~ 20 Ma between 85°W and 93°W (Figs. 4A and B), representing the failure of the weak and young subducting plate due to sub-slab overpressure. This process coincides with the mid-Miocene ignimbrite flare up event in Central America (Sigurdsson et al., 1997; Leckie et al, 2000) and is also similar to what occurred within the Farallon slab during the mid-Miocene, where the slab tear below Oregon and Nevada led to abrupt surface uplift, upwelling within the mantle wedge, and the development of the Columbia River flood basalts (Liu and Stegman, 2012). The observed high topography and low Bouguer gravity (Fig. S1) above the predicted slab gap in the study area further support this model result.

ONGOING FRAGMENTATION OF THE COCOS SLAB AND ITS

GEODYNAMIC IMPLICATIONS

95

96

97

98

99

100

101

102

103

104

105

106

107

108

109

110

111

112

113

114

115

116

117

The realization of a fragmenting Cocos slab that is pervious to mantle flow can reconcile multiple lines of seemingly contradictory observations. For example, seismic tomography revealed a broken or significantly weakened upper-mantle slab (Rogers et al., 2002; Zhu et al., 2020). In contrast, the existence of intermediate depth earthquakes and VF volcanoes are inconsistent with the existence of a slab window. According to both our simulated present slab geometry (Fig. 4D), inferences of seismic anisotropy (Fig. 3), as well as the area of low Bouguer

gravity anomalies (Fig. S1), the fragmented portion of the Cocos slab has an along-trench dimension of about 700 km, approximately between 86°W and 93°W. In our model, this slab fragmentation starts at about 60 km depth, immediately beneath the lithosphere of the overriding plate, as is confirmed by the observation that the anisotropy-indicated flow systems below ~80 km in the sub-slab region and the mantle wedge show a high degree of continuity (Zhu et al., 2020) (Fig. S3). The maximum depth of the intensively fractured portion is about 200 km, as this is the depth of suddenly thickened slab thermal structure (Fig. 4E) and increased seismic velocity anomalies (Zhu et al., 2020) (Fig. 4F and Fig. S2). This is also the depth below which the earthquake productivity becomes similar to subduction zones globally (Fig. 2B).

The intensively fractured section of the Cocos slab above 200 km depth is mechanically weaker and warmer than a normal slab due to the strong internal deformation associated with ongoing fragmentation (Fig. 4). Consequently, this slab portion should have a lower earthquake productivity (Fig. 2B). Both the reduced mechanical strength and higher temperature of the intensively fractured portion of the slab may also be responsible for the slightly positive velocity anomaly relative to the deeper portion as revealed by seismic tomography (Zhu et al., 2020). This portion of the slab can still carry a sufficient amount of hydrous phases to produce the VF volcanoes. Meanwhile, the sub-slab mantle material, which is under enhanced dynamic pressure and has a higher temperature than that in the mantle wedge (Blackwell et al., 1990) (thus more buoyant), actively migrates upward through the tearing slab hinge to produce the higher-thannormal heat flow, anomalously high elevation, low Bouguer gravity anomalies (Fig. S1), and the BVF volcanoes.

REFERENCES CITED

142	Abt, D. L., Fischer, K. M., Abers, G. A., Protti, M., González, V., & Strauch, W. (2010).
143	Constraints on upper mantle anisotropy surrounding the Cocos slab from SK (K) S
144	splitting. Journal of Geophysical Research: Solid Earth, 115(B6).
145	Baier, J., Audétat, A. and Keppler, H., 2008. The origin of the negative niobium tantalum
146	anomaly in subduction zone magmas. Earth and Planetary Science Letters, 267(1-2),
147	pp.290-300.
148	Bernal-López, L. A., Garibaldi, B. R., Soto, G. L., Valenzuela, R. W., & Escudero, C. R. (2016).
149	Seismic anisotropy and mantle flow driven by the Cocos slab under southern Mexico.
150	Pure and Applied Geophysics, 173(10-11), 3373-3393.
151	Bird, P. (2003). An updated digital model of plate boundaries. Geochemistry, Geophysics,
152	Geosystems, 4(3).
153	Blackwell, D. D., Steele, J. L., & Carter, L. C. (1990). Heat flow patterns of the North American
154	continent: A discussion of the DNAG geothermal map of North America. DOEEEGTP
155	(USDOE Office of Energy Efficiency and Renewable Energy Geothermal Tech Pgm).
156	Borgeaud, A. F., Kawai, K., & Geller, R. J. (2019). Three-dimensional S velocity structure of
157	the mantle transition zone beneath Central America and the Gulf of Mexico inferred
158	using waveform inversion. Journal of Geophysical Research: Solid Earth, 124(9), 9664-
159	9681.
160	Carr, M. J. (1984). Symmetrical and segmented variation of physical and geochemical
161	characteristics of the Central American volcanic front. Journal of Volcanology and
162	Geothermal Research, 20(3-4), 231-252.

163 Carr, M. J., Feigenson, M. D., Bolge, L. L., Walker, J. A., & Gazel, E. (2014). RU CAG eochem, a database and sample repository for Central American volcanic rocks at 164 Rutgers University. Geoscience Data Journal, 1(1), 43-48. 165 Carr, M. J., & Pontier, N. K. (1981). Evolution of a young parasitic cone towards a mature 166 central vent; Izalco and Santa Ana volcanoes in El Salvador, Central America. Journal of 167 Volcanology and Geothermal Research, 11(2-4), 277-292. 168 Castellanos, J., Pérez-Campos, X., Valenzuela, R., Husker, A., & Ferrari, L. (2017). Crust and 169 upper-mantle seismic anisotropy variations from the coast to inland in central and 170 Southern Mexico. Geophysical Journal International, 210(1), 360-374. 171 Dougherty, S. L., Clayton, R. W., & Helmberger, D. V. (2012). Seismic structure in central 172 Mexico: Implications for fragmentation of the subducted Cocos plate. Journal of 173 Geophysical Research: Solid Earth, 117(B9). 174 Hess, H. H. (1964). Seismic anisotropy of the uppermost mantle under oceans. Nature, 175 203(4945), 629-631. 176 Idárraga-García, J., Kendall, J. M., & Vargas, C. A. (2016). Shear wave anisotropy in 177 northwestern South America and its link to the Caribbean and Nazca subduction 178 geodynamics. Geochemistry, Geophysics, Geosystems, 17(9), 3655-3673. 179 180 Kong, F., Gao, S. S., Liu, K. H., Fang, Y., Zhu, H., Stern, R. J., & Li, J. (2022). Metastable olivine within oceanic lithosphere in the uppermost lower mantle beneath the eastern 181 United States. Geology. 182 183 Leckie, R.M., Sigurdsson, H., Acton, G.D., and Draper, G. (Eds.), 2000. Proc.ODP, Sci. Results, 165: College Station, TX (Ocean Drilling Program). 184

185 Liu, L. and D.R. Stegman (2011), Segmentation of Farallon slab, Earth Planet. Sci. Lett. 311, 1-10. 186 Liu, L. and D.R. Stegman (2012), Origin of Columbia River flood basalt controlled by 187 propagating rupture of the Farallon slab, Nature, 482, 386-389. 188 Long, M. D., & Silver, P. G. (2009). Mantle flow in subduction systems: The subslab flow field 189 and implications for mantle dynamics. Journal of Geophysical Research: Solid Earth, 190 114(B10). 191 Masy, J., Niu, F., Levander, A., & Schmitz, M. (2011). Mantle flow beneath northwestern 192 Venezuela: Seismic evidence for a deep origin of the Mérida Andes. Earth and Planetary 193 Science Letters, 305(3-4), 396-404. 194 McDonough, W. F., & Sun, S. S. (1995). The composition of the Earth. Chemical geology, 195 120(3-4), 223-253. 196 Pardo, M., & Suárez, G. (1995). Shape of the subducted Rivera and Cocos plates in southern 197 Mexico: Seismic and tectonic implications. Journal of Geophysical Research: Solid 198 Earth, 100(B7), 12357-12373. 199 Patino, L. C., Carr, M. J., & Feigenson, M. D. (2000). Local and regional variations in Central 200 American arc lavas controlled by variations in subducted sediment input. Contributions to 201 Mineralogy and Petrology, 138(3), 265-283. 202 Piñero-Feliciangeli, L. T., & Kendall, J. M. (2008). Sub-slab mantle flow parallel to the 203 204 Caribbean plate boundaries: Inferences from SKS splitting. Tectonophysics, 462(1-4),

22-34.

- Porritt, R. W., Becker, T. W., & Monsalve, G. (2014). Seismic anisotropy and slab dynamics
 from SKS splitting recorded in Colombia. Geophysical Research Letters, 41(24), 87758783.
- Rogers, R. D., Kárason, H., & van der Hilst, R. D. (2002). Epeirogenic uplift above a detached slab in northern Central America. Geology, 30(11), 1031-1034.
- Rose Jr, W. I., & Stoiber, R. E. (1969). The 1966 eruption of Izalco volcano, El Salvador.
- Journal of Geophysical Research, 74(12), 3119-3130.
- Russo, R. M., & Silver, P. G. (1994). Trench-parallel flow beneath the Nazca plate from seismic
- anisotropy. Science, 263(5150), 1105-1111.
- Sigurdsson, H., Leckie, R.M., Acton, G.D., et al., 1997. Proc. ODP, Init. Repts., 165: College Station, TX (Ocean Drilling Program).
- Silver, P. G., & Chan, W. W. (1991). Shear wave splitting and subcontinental mantle deformation. Journal of Geophysical Research: Solid Earth, 96(B10), 16429-16454.
- van Benthem, S., Govers, R., Spakman, W., & Wortel, R. (2013). Tectonic evolution and mantle structure of the Caribbean. Journal of Geophysical Research: Solid Earth, 118(6), 3019-
- 221 3036.
- Walker, J. A., Carr, M. J., Patino, L. C., Johnson, C. M., Feigenson, M. D., & Ward, R. L.
- 223 (1995). Abrupt change in magma generation processes across the Central American arc in
- southeastern Guatemala: Flux-dominated melting near the base of the wedge to
- decompression melting near the top of the wedge. Contributions to Mineralogy and
- Petrology, 120(3), 378-390.

Walker, J. A., Patino, L. C., Cameron, B. I., & Carr, M. J. (2000). Petrogenetic insights provided by compositional transects across the Central American arc: Southeastern Guatemala and Honduras. Journal of Geophysical Research: Solid Earth, 105(B8), 18949-18963. Walker, J. A., Teipel, A. P., Ryan, J. G., & Syracuse, E. (2009). Light elements and Li isotopes across the northern portion of the Central American subduction zone. Geochemistry, Geophysics, Geosystems, 10(6). Zhou, Q., Hu, J., Liu, L., Chaparro, T., Stegman, D. R., & Faccenda, M. (2018). Western US seismic anisotropy revealing complex mantle dynamics. Earth and Planetary Science Letters, 500, 156-167. Zhu, H., Stern, R. J., & Yang, J. (2020). Seismic evidence for subduction-induced mantle flows underneath Middle America. Nature communications, 11(1), 1-12.

ACKNOWLEDGMENTS

The seismic data used in this study were obtained from the Incorporated Research Institutions for Seismology Data Management Center (https://ds.iris.edu/ds/nodes/dmc/). The original version of CitcomS is available at https://geodynamics.org/. This study was supported by the National Science Foundation (grants 1321656 to K. Liu, grants 1554554 to L. Liu, and grants 1830644 to K. Liu).

Supplemental Material. Figures S1 – S5 (bouguer gravity anomalies and focal mechanism solutions; cross-section of tomographic images and anisotropy beneath Central America; isotropic S-wavespeed anomalies and azimuthal anisotropy; azimuthal equidistant map; shear wave splitting measurement examples) Table S1 (model parameters).

Figure Captions:

Fig. 1. Tectonic setting of northern Central America. The brown squares show the seismic stations used in the study. The red triangles represent arc-front volcanoes, the black triangles represent back-arc volcanoes, and the colored dots represent the epicenters and focal depths of Magnitude 4.5 and greater earthquakes that occurred between 1980 and 2022. The yellow contour lines show the depths of the Cocos slab. The area outlined by the dashed lines indicates the approximate extent of the proposed pervious slab. The enclosed region in the inset map shows the study area, where the contour lines show the ocean floor ages. The red bars represent results from previous and the present shear wave splitting studies (Abt et al., 2010; Bernal-López et al., 2016; van Benthem et al., 2013; Russo and Silver, 1994; Masy et al., 2011; Porritt et al., 2014; Idárraga-García et al., 2016; Castellanos et al., 2016; Piñero-Feliciangeli and Kendall, 200813, 14, 19-25). The orientations of the bars show the fast polarization orientation, and the length of the bars is proportional to the splitting time. Plate boundaries from (Bird, 2003).

Fig. 2. Chemical composition and earthquake distribution. (A) BVF and VF average diagrams with data (Rose and Stoiber, 1969; Carr and Pontier, 1981; Carr, 1984; Walker et al., 1995; Walker et al., 2000; Patino et al., 2000; Walker et al., 2009; Carr et al., 2014). Primitive mantle values are from (McDonough and Sun, 1995). (B) Depth variation of the number of M4.0 and greater earthquakes that occurred between 2010 and 2022 for northern Central America (red) and the whole Earth (blue). The numbers were normalized by the corresponding value at 60 km depth.

Fig. 3. Results from shear wave splitting analysis. Individual splitting measurements (red bars) from this study plotted at the stations and above the ray-piercing points at 50 km depth. The area outlined by the dashed lines indicates the approximate extent of the proposed pervious slab.

Fig. 4. Modeled Cocos subduction and present slab geometry. (a) Map view slab evolution at 160 km depth from 40 Ma to the present. Colored translucent patterns show slab interiors (400 °C colder than the ambient mantle). (b) Present slab geometry at 206 km depth, with color contours outlining the major slab gap at different depths. (c-e) Cross sectional view of subduction along A-A' shown in B at different times. Green contours represent the -400 °C isotherm anomaly. (f) Seismic image of present slab structure along A-A' [see (Zhu et al., 2020)

and references therein].

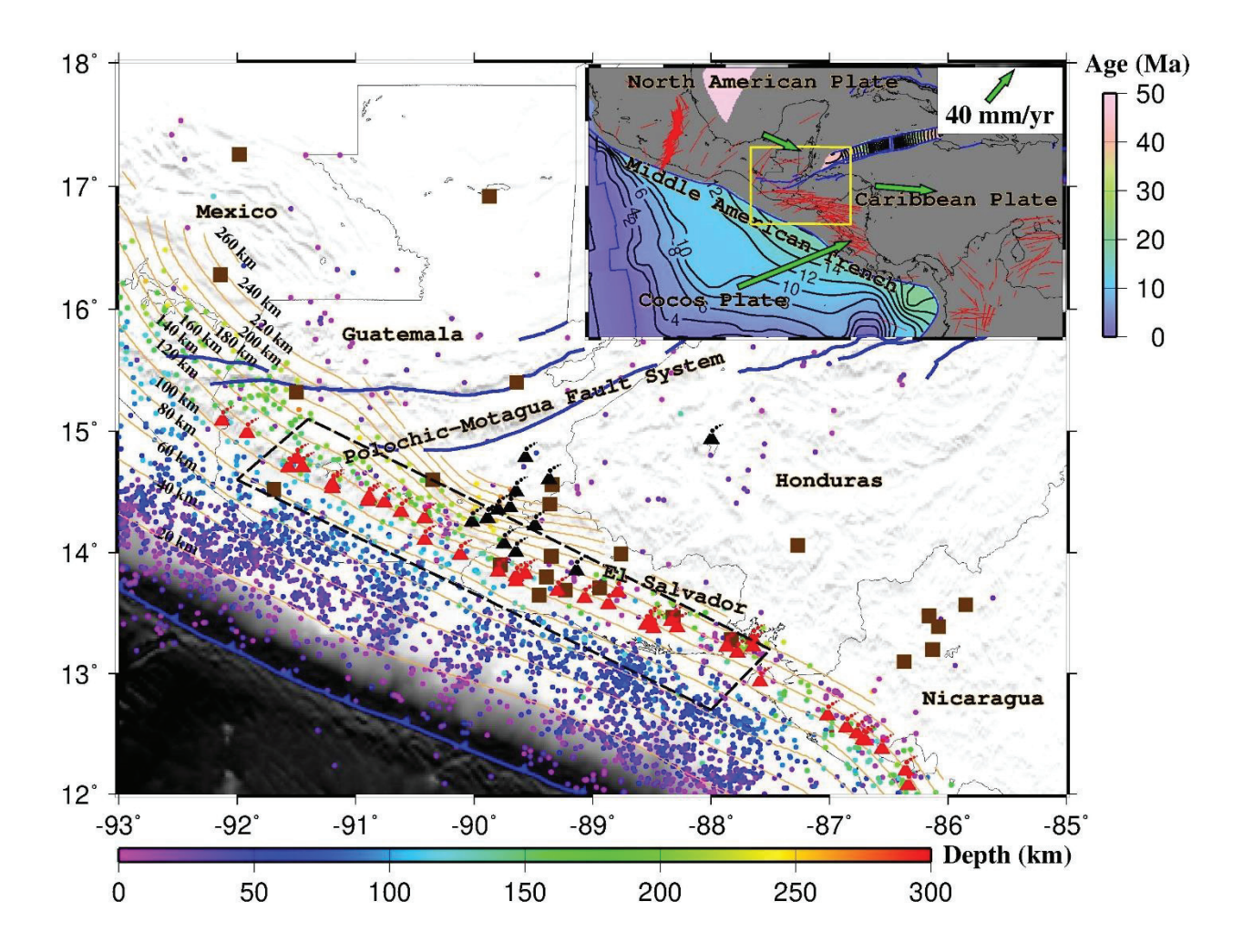


Figure 2

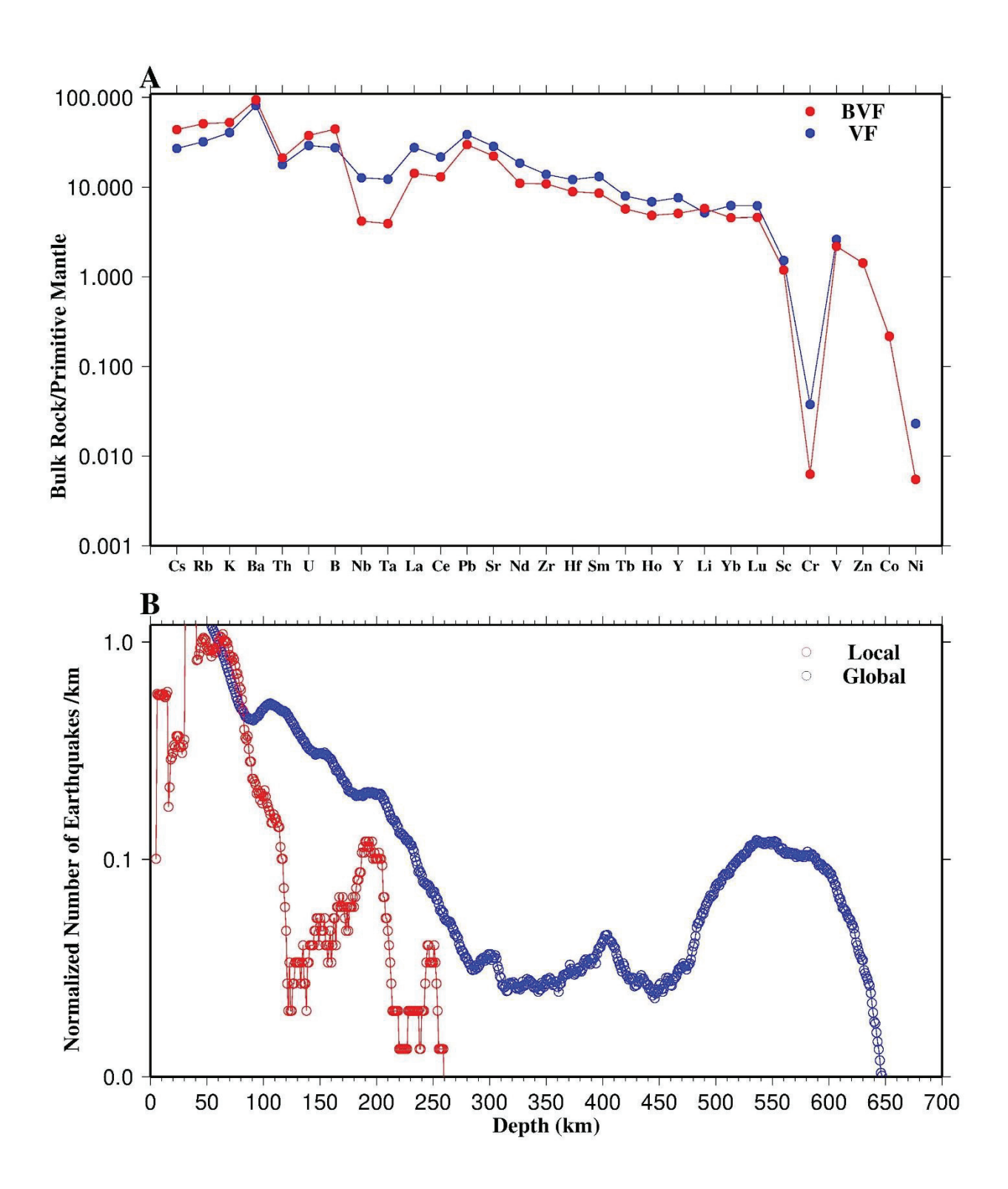


Figure 3

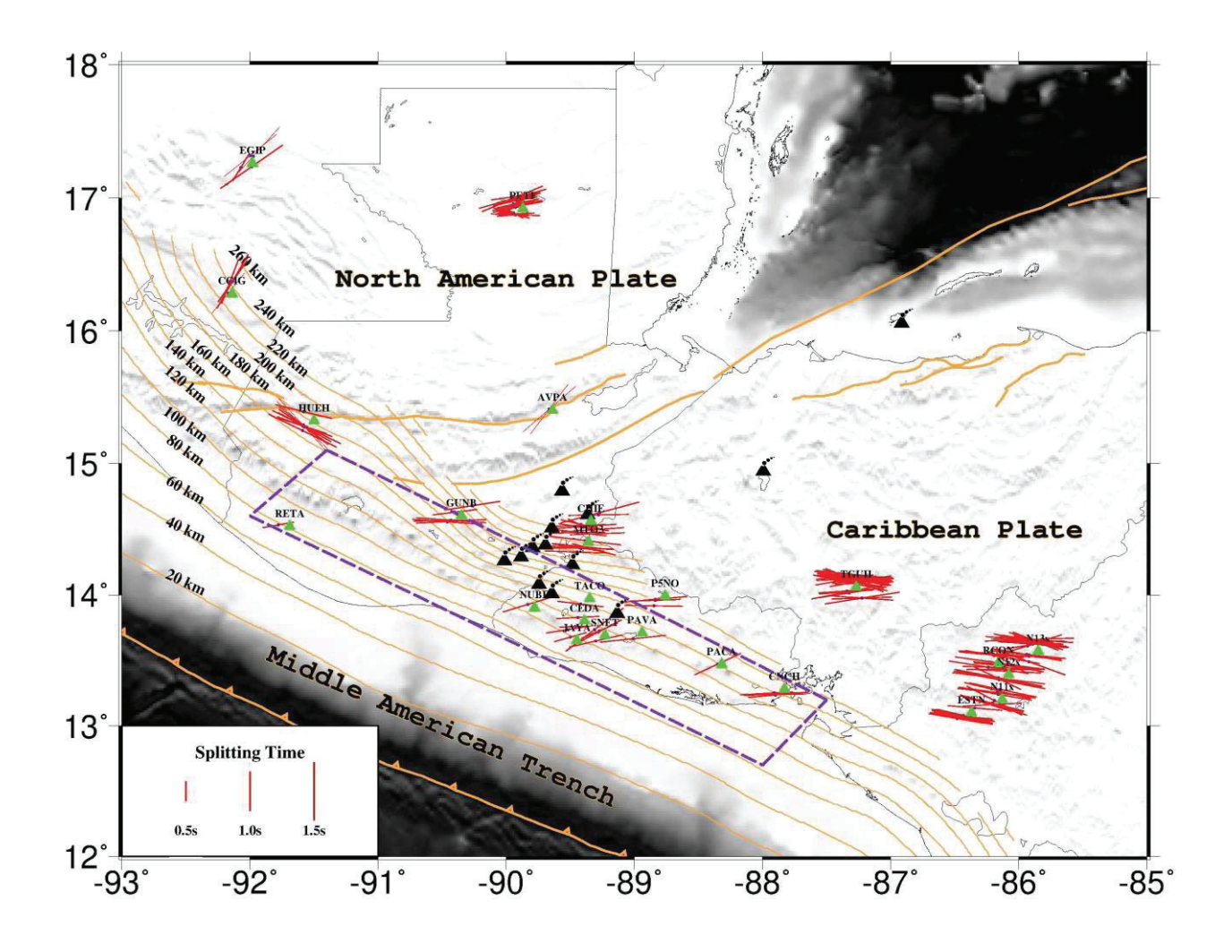


Figure 4

